PHYSICAL REVIEW B VOLUME 32, NUMBER 10 15 NOVEMBER 1985

Structural and dynamical behavior of noble-gas surfaces

W. Schommers
Institut für Nukleare Festkörperphysik, Kernforschungszentrum Karlsruhe GmbH., Postfach 3640, D-7500 Karlsruhe, Federal Republic of Germany
(Received 11 February 1985)

Molecular-dynamics calculations have been performed for noble-gas (krypton) surfaces. As pair potential between the particles, we used the potential of Barker *et al.* This potential is consistent with a wide range of experimental data and should be more realistic than the more familiar Lennard-Jones (6-12) potential. The calculations have been performed for temperatures of 7, 70, and 102 K. We used the following model: The krypton atoms are arranged as a slab-shaped fcc crystal, the two free surfaces being (100) planes. The slab consists of 11 layers of 50 atoms, i.e., the total number of particles used in the calculations was 550. The structure of the layers has been studied by means of the single-particle distribution function and the pair correlation function. Whereas the results for the *innermost* layer of the model agree well with the corresponding data of the bulk, there are relatively large effects for the *outermost* layer. This is also the case for the mean-square displacements $\langle u^2 \rangle$, which is much larger in the outermost layer than in the bulk of the crystal. For $T = 102$ K, we observe the effect of surface premelting: The outermost layer is disordered and the particles perform a diffusive motion parallel to the surface and the diffusion coefficient D is comparable to that in liquids. The effect of premelting in our system is obviously much more pronounced than in the case of Lennard-Jones systems.

I. INTRODUCTION

In this paper we want to study the structure and the dynamics of free crystal surfaces. The knowledge of the structural and the dynamical behavior of such surfaces is also important for the understanding of phenomena at the surface. For example, the behavior of adsorbates and chemical reactions at surfaces are influenced by these properties.

In order to carry out a first-principles calculation of surface properties, it is necessary to have an accurate knowledge of the atomic interactions. The only group of materials for which this requirement is nearly satisfied is that of noble-gas solids. In contrast to metals, the potential functions of noble-gas solids do not depend on the density, and they are the same at the surfaces and in the bulk of the crystal. At free metal surfaces the local background electron density may be changed from its average bulk value and produces concomitant changes in the potential functions. Such difficulties do not arise at noble-gas surfaces and, therefore, we want to restrict our study to noble-gas (krypton) surfaces.

It is widely accepted that in the quantitative treatment of the surface phenomena *anharmonic* effects have to be taken into consideration. This is because the mean-square amplitudes of the particles are significantly larger at the surface of the crystal than in the bulk. The harmonic approximation should be valid[1] for surface vibrations of noble-gas crystals below one-sixth of the melting temperature T_m (as compared to about $\frac{1}{3}T_m$ for the bulk). The melting temperature of krypton is 116 K. Thus, in the case of krypton usual *lattice-dynamics* calculations should only be valid for $T < 19$ K. For $T > 19$ K we have to consider *anharmonic* effects. *Molecular-dynamics* (MD) calculations are important in studying classical many-particle systems with strong anharmonicities, since anharmonicity is treated without approximations. In this paper we want to study by means of MD the structure and dynamics of a krypton surface as a function of temperature. Because we use MD we are not restricted to temperatures smaller than 19 K as in the case of usual lattice-dynamics calculations.

Because the surface particles are, in general, less bonded than the bulk particles, we expect that the structure and the dynamics are more sensitive to variations in temperature than in the bulk of the crystal. Thus, in the study of temperature effects (e.g., phase transitions) of *adsorbed* layers, also the crystal surface on which the layer is situated should be treated as temperature dependent and not as a *static* lattice corresponding to a temperature of zero. Recently, the temperature dependence of the structure of adsorbed layers has been investigated by MD.[2–4] In Refs. 2 and 3 a monolayer is situated on a *static* crystal surface. We want to study here in a first step the microscopic behavior of crystal surfaces without the presence of adsorbed particles.

We have chosen a *krypton* system because for this substance a reliable pair potential[5] is available. The krypton potential of Barker *et al.*[5] should be more realistic than the more familiar Lennard-Jones (6-12) potential because it undoubtedly correlates accurately a much wider range of experimental data. We shall see in Sec. III that the differences between Barker's potential and the Lennard-Jones potential give rise not only to quantitative effects in the results of surface properties, but also to *qualitative* effects. All MD calculations on noble-gas surfaces reported in literature have been done exclusively with the Lennard-Jones potential. Examples are given in Refs.

2—4 and in Ref. 6.

The main topics of this work are (i) interplanar spacings (relaxation) and the structure perpendicular to the surface, (ii) pair correlation functions parallel to the surface, (iii) mean-square displacements perpendicular and parallel to the surface, and (iv) nonlinear effects. Because Barker's potential for krypton is close to the real pair potential, the results given in this paper can be considered a quantitative description. Some of these results have been briefly described in a preliminary publication.[7]

II. MODEL AND INTERACTION POTENTIAL

A. Model parameter

Our MD calculations have been performed for the following model: The krypton atoms are arranged as a slab-shaped fcc crystal, the two free surfaces being (100) planes. For this (100) surface, which is an open, square lattice, the effect of premelting should be more pronounced than at the (111) close-packed triangular surface. The slab consists of 11 layers of 50 atoms, i.e., the total number of particles used in the calculations was 550. Periodical boundary conditions (PBC's) were imposed with respect to translations parallel to the surface. For this system the classical Hamiltonian equations were solved by iteration. The time step used in the calculation was 10^{-14} sec. We did the calculations for 8500 time steps (0.85×10^{-10} sec). The magnitude of the initial velocities of all atoms was chosen to be equal, but Maxwell's distribution was reached after 120 time steps (1.2×10^{-12} sec). The initial directions of the velocities have been distributed randomly, so that the velocity averaged over all atoms is zero and remains zero for all time steps.

It is widely accepted[8] that for potentials whose range is shorter than half the box size, the effect of PBC's will be rather small. In the case of our krypton system the box size is $L=28.5$ Å and the cutoff radius for the potential (the details of the potential are given in Sec. II B) was chosen to be the fourth-nearest-neighbor distance (8 Å); we found that the interaction of the fifth neighbors has no influence on the results. Thus, we may conclude that the krypton pair potential is short ranged compared to half the box size and, therefore, the effects due to PBC's should be small. This is confirmed by a more systematic analysis: We varied the particle number from 108 to 864 and found that in the case of $N=550$ no systematic effects arose out of PBC's.

All the bulk data which are given in this paper have been determined also by MD (model without free surfaces, i.e., PBC's in all directions) using the same model parameter and the same interaction potential as in the surface calculations.

We did the calculations for three temperatures: 7, 70, and 102 K (the melting temperature is 116 K). The density for each temperature has been extracted from the experimental data given in Ref. 9.

B. Interaction potentials for krypton

For the description of the interaction between the particles, in general, not only the *pair* potential has to be considered but also *many-body* forces. For example, it is shown in Refs. 10—12 that the influence of *three-body* forces on *dynamical* correlation functions can be of importance. So, the potential energy U for N identical atoms has to be expanded in terms of pair and many-body contributions:

$$U=\tfrac{1}{2}\sum_{\substack{i,j=1\\ i\neq j}}^{N} u_{ij}+\tfrac{1}{6}\sum_{\substack{i,j,k=1\\ i\neq j\neq k}}^{N} u_{ijk}+\cdots . \tag{1}$$

Clearly, the most important term in Eq. (1) is the pair-potential contribution. For the pair potential $u_{ij}\equiv u(r_{ij})$, where r_{ij} is the relative distance between the particles i and j, we have chosen the potential of Barker *et al.*,[5] which is shown in Fig. 1. In order to check whether many-body contributions are relevant, we have added the Axilrod-Teller three-body potential[13]

$$u_{ijk}=\nu\frac{1+3\cos\theta_1\cos\theta_2\cos\theta_3}{r_{ij}^3 r_{ik}^3 r_{jk}^3} \tag{2}$$

to Barker's pair potential. r_{ij},r_{ik},r_{jk} and $\theta_1,\theta_2,\theta_3$ are the sides and the angles of the triangle formed by the particles i, j, and k. The parameter ν was chosen to be 220.4×10^{-84} cm^{9}erg (see Ref. 14); the investigations in Ref. 12 indicate that this value is realistic for krypton. On the basis of this model we have studied in a first step how u_{ijk} is reflected in the *phonon density of states* (PDOS) for the bulk of krypton. Due to the three-body interactions the computer-time requirements are very large and we had to restrict ourselves to a system consisting of 108 particles; similar calculations are planned for systems with free surfaces on the basis of more than 108 particles.

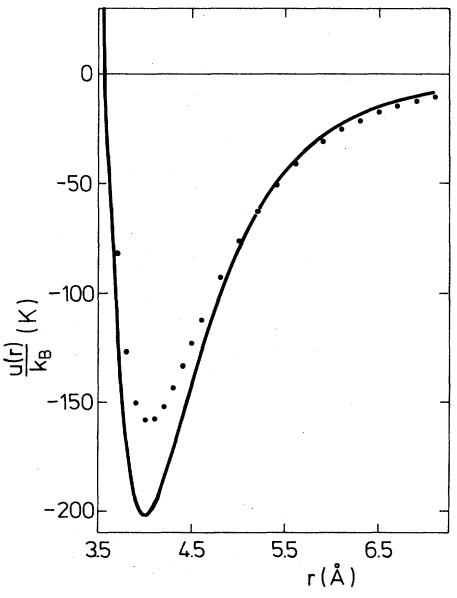

FIG. 1. Pair potentials for krypton: ——, potential of Barker *et al.*; · · · ·, Lennard-Jones (6-12) potential.

The PDOS $f(\omega)$ has been obtained by Fourier transform of the velocity autocorrelation function (VAF),

$$\psi(t)=\frac{\langle \mathbf{v}_i(t_0)\cdot\mathbf{v}_i(t+t_0)\rangle}{\langle \mathbf{v}_i(t_0)^2\rangle}\ , \tag{3}$$

where the average $\langle\cdots\rangle$ is performed over time origins t_0 and particles i. The number of time origins was chosen to be 200. Then we obtain a statistical error ($i=108$) of 0.7%. The PDOS is given in terms of $\psi(t)$ by

$$f(\omega)=\frac{2}{\pi}\int_0^\infty \psi(t)\cos(\omega t)dt\ , \tag{4}$$

where $f(\omega)$ is normalized to unity. In the calculation of $f(\omega)$ one is limited to a finite range of the time t, and it is necessary to truncate the integration at $t=t'<\infty$. We performed each calculation for 10 values of t', and the resulting spectra do not show systematic deviations from each other. A possibility for a quantitative estimation of the error due to the cutoff effect in t is to integrate the spectrum: $f(\omega)$ is normalized to unity and we found that the deviations of our integrated data from unity are not larger than 6%. MD results for the PDOS in the bulk of krypton at $T=7$ K with and without the presence of three-body interactions are plotted in Fig. 2. It can be seen from Fig. 2 that the effect of the three-body forces is relatively small—much smaller than in the case of gaseous krypton,[12] but larger than the error in the calculations. The arrows in Fig. 2 indicate the positions of the peaks in $f(\omega)$ which have been obtained on the basis of a three-nearest-neighbor force-constant fit to experimental dispersion curves.[15] The positions of the peaks obtained from our calculations are the same, indicating that already a small system consisting of 108 particles is able to give a realistic description. It should be mentioned that quantum effects (not considered in our calculation) should, in principle, also contribute, but these are expected to be relatively small in the case of krypton (see Refs. 14 and 16).

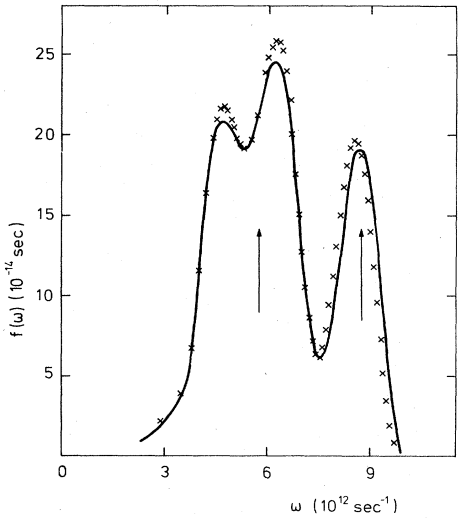

FIG. 2. Phonon density of states in the bulk of krypton at 7 K: ——, with three-body forces; ×××, without three-body forces.

In conclusion, the effect of three-body interactions on the PDOS is small and, therefore, we restricted ourselves in Eq. (1) to the pair-potential contribution.

The pair potential of Barker *et al.*[5] (Fig. 1) is consistent with a wide range of experimental data, including second virial coefficients, gas-transport properties, solid-state data, and measurements of differential scattering cross sections. The more familiar Lennard-Jones potential is also shown in Fig. 1. Although the shapes of the two potentials are similar, there are considerable quantitative differences. For example, the depth of the minimum of Barker's potential is approximately 25% larger than the depth of the Lennard-Jones potential. The potential of Barker *et al.* should be more realistic because it undoubtedly correlates accurately a much wider range of experimental data. We did an additional check for the potential of Barker *et al.* on the basis of very accurate structure data for gaseous krypton.[17] It turned out (see Ref. 7) that Barker's potential describes the experimental structure data undoubtedly better than the Lennard-Jones potential.

In the calculation of the properties of the system the forces acting on the particles are relevant. The force $\mathbf{F}_i$ acting on particle i is given by

$$\mathbf{F}_i=-\sum_{\substack{j=1\\ j\neq i}}^{N}\frac{\mathbf{r}_{ij}}{r_{ij}}\frac{\partial u(r_{ij})}{\partial r_{ij}}\ , \tag{5}$$

where $u(r_{ij})\equiv u_{ij}$ with $r_{ij}\equiv r$. Thus, the derivative of different pair potentials should be studied. In Fig. 3, $\partial u(r)/\partial r$ are plotted as well for Barker's potential as for the Lennard-Jones potential in the vicinity of the first-nearest-neighbor distance; the first-nearest-neighbor contribution to the sum in Eq. (5) should be of considerable relevance. It can be seen from Fig. 3 that the differences between the derivatives of the two potentials are very large for all temperatures.

The differences between Barker's potential and other realistic pair potentials (for example, the potential of Aziz[18]) are very small—much smaller than the differences

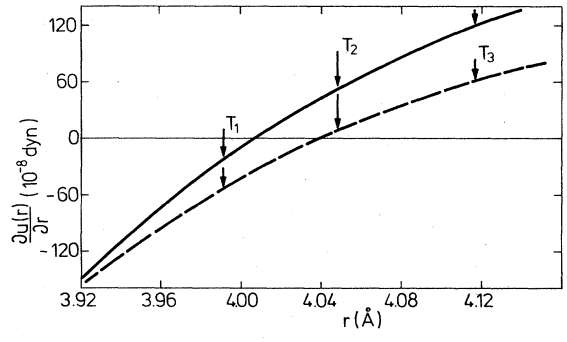

FIG. 3. The derivative of pair potentials in the vicinity of the first-nearest-neighbor distance. The position of the arrows are the first-nearest-neighbor distances at $T_1=7$ K, $T_2=70$ K, and $T_3=102$ K: ——, Barker's potential; — — —, Lennard-Jones potential.

between Barker's potential and the Lennard-Jones potential. So, we expect that the potential of Aziz will also give reliable results for the properties of the system.

III. RESULTS

A. Structure and displacements perpendicular to the surface

In the following the coordinates x,y are parallel to the surface and the coordinate z is the direction perpendicular to the surface. Furthermore, we define $m=1$ for the outermost layer, $m=2$ for the plane just below the upper layer, and so on. In order to investigate how the particles are distributed in the z direction, we have calculated the *single-particle distribution function* $g_1(z)$; $g_1(z)$ is the probability that a particle of the system is between z and $z+dz$. The results for $g_1(z)$ for the temperatures of 7, 70, and 102 K are shown in Fig. 4. It can be seen from Fig. 4 that the single-particle distribution for $m=6$ (innermost layer) agrees very well for all temperatures with the corresponding data of the bulk. There are, however, large effects in the outmost layer ($m=1$): with decreasing m the height of the peaks are getting smaller and their width broader. This is consistent with the fact that the mean-square amplitudes of the particles are significantly larger at the surface than in the bulk of the crystal; the MD results of the mean-square amplitudes are shown in Fig. 5.

In the calculation for $T=7$ K we observe a *double-peak structure* which is a typical feature of a classical oscillator; it is not due to double minima in the effective single-particle potential, but rather to a dynamic effect which will be discussed in more detail in a forthcoming paper. For $m=5$ and $m=6$ this double-peak structure could not be resolved by our MD calculation and this is because the amplitudes of the oscillations are very small for $m=5$ and $m=6$ [0.07 Å for $m=6$ (see Fig. 5)]. The *asymmetry* in the peak structure for $m=1$ can be explained as follows: Let us consider surface particles which are vibrating perpendicular to the surface. Upon moving inward, they collide with the particles of the second layer ($m=2$) and the *repulsive* part of the potential is effective, which causes them to reverse their direction of motion. When the particles are moving outward, however, they do not collide with any other particles, but the direction of motion is reversed by the *attractive* part of the potential in the crystal. Because of the asymmetry of the repulsive and the attractive parts of the pair potential, we observe an asymmetry in the probability distribution described here by the single-particle distribution function $g_1(z)$ [Fig. 4(a), $m=1$].

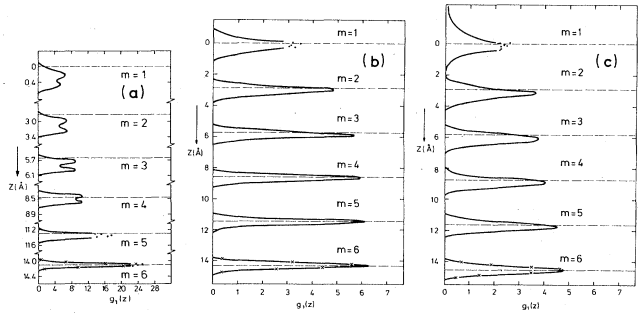

FIG. 4. Single-particle distribution functions at (a) $T=7$ K, (b) $T=70$ K, and (c) $T=102$ K. Solid lines and points, $g_1(z)$ at the surface; crosses, $g_1(z)$ in the bulk; dashed lines, mean positions of the layers in the bulk of the crystal.

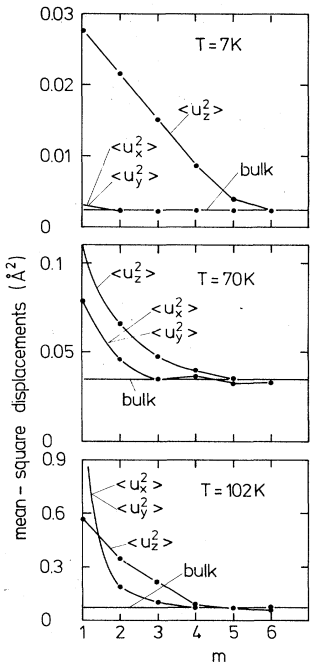

FIG. 5. Mean-square displacements for different layers and temperatures.

Because the attractive part is weaker than the repulsive part of the potential, the probability of finding a particle in the region where the potential is attractive is larger than that of finding it in the repulsive region. The double-peak structure could not be recognized in the calculations for 70 and 102 K, indicating that the layers are disturbed perpendicular to the surface; there must be a thermally induced *disorder*.

Behavior of the root-mean-square displacements: From Fig. 5 we observe that the gradient of the root-mean-square displacements $\langle u_z^2\rangle^{1/2}$ in the *bulk* decreases with increasing temperature. *Explanation*: the *repulsive* part of the pair potential is becoming effective with increasing temperature and, therefore, the gradient of $\langle u_z^2\rangle^{1/2}$ in the *bulk* as a function of temperature must decrease with increasing temperature. At low temperatures ($T<75$ K; the value of 75 K has been obtained by extrapolation) the gradient of $\langle u_z^2\rangle^{1/2}$ at the *surface decreases* with increasing temperature. For $T>75$ K, however, the gradient of $\langle u_z^2\rangle^{1/2}$ at the *surface increases* with increasing temperature. *Explanation*: when a *surface* particle is moving *outward* it is not influenced by the repulsive part of the po-

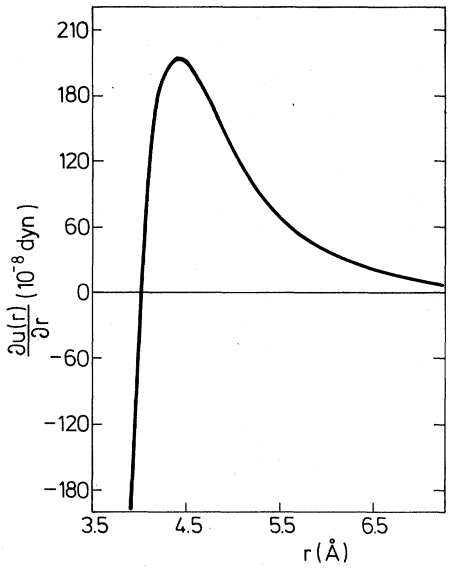

FIG. 6. Derivative of Barker's pair potential.

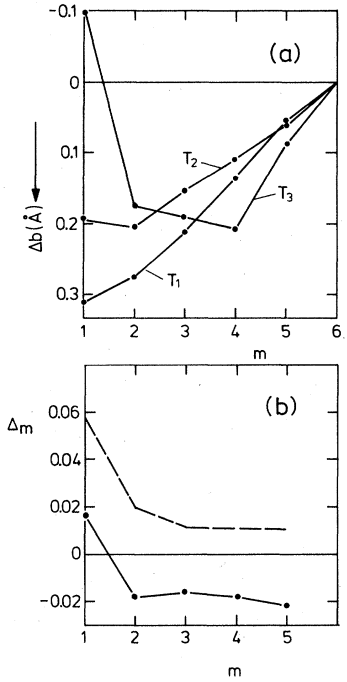

FIG. 7. (a) The deviations of the mean positions of layers near the surface from the mean position that these layers would have in the bulk. Δb is defined by Eq. (6). (b) Interplanar spacing of surface layers. Δ_m is defined by Eq. (7): ——, our model ($T=70$ K); — — —, Lennard-Jones system (Ref. 6) ($T=57$ K).

tential but by its attractive part, and the derivative of the pair potential (see Fig. 6), which determines the forces acting on the particles [see Eq. (5)], has a maximum (at 4.43 Å) in the attractive region. At low temperatures ($T<75$ K) the distance of most of the particles of the outermost layer from those of the second layer is smaller than 4.43 Å and—as in the case of repulsion—the gradient $\langle u_z^2\rangle^{1/2}$ as a function of temperature *decreases* with increasing T. At 102 K, however, distances with $r>4.43$ Å are probable and we expect that the gradient of $\langle u_z^2\rangle^{1/2}$ increases for $T>102$ K.

B. Interplanar spacings

Let us now study the deviations of the mean positions a_m' of layers near the surface from the mean positions a_m that these layers would have in the bulk of the crystal. a_m' can be obtained from the single-particle distribution function $g_1(z)$ (see Fig. 4). a_m' is given by the position of the center of mass of the peak belonging to layer m. In the case of a symmetrical curve, a_m' is identical to the position of the maximum of the peak. In Fig. 7 the quantity

$$\Delta b = a_m' - a_m \tag{6}$$

is represented as a function of m. It can be seen from Fig. 7 that there is a *multilayer* relaxation for all three temperatures. In the case of $T_1=7$ K the relaxation effect is getting small with increasing m. Due to the geometrical symmetry the mean position of the innermost layer ($m=6$) must be identical to that in the bulk of the crystal; this is fulfilled for 7, 70, and 102 K.

In general, the relaxation as a function of temperature is determined by minimizing the total free energy (including vibrational modes), and the resulting mean displacements a_m' are called the *dynamic displacements*. If the mean displacements are determined by minimizing the static energy, we only obtain the *static displacements*. Most of the lattice-dynamical calculations in literature (see, for example, Ref. 19) have been performed on the basis of the *static* displacements. However, it is shown in Fig. 7 that Δb varies strongly with temperature, and therefore, the assumption that the mean displacements have their static values breaks down at high temperatures. Thus, in lattice-dynamical calculations we have to consider that *both* the *harmonic* approximation and the validity of the *static* approximation for the mean displacements break down at high temperatures. MD calculations take both dynamic displacements and anharmonic effects into account automatically. The curves in Fig. 7 show the *dynamic* displacements. We expect, however, that the curve for $T_1=7$ K is close to the *static* case.

Let us compare our results with those obtained from a Lennard-Jones system.[6] In Ref. 6 the results of the quantity

$$\Delta_m = \frac{a_{m+1}' - a_m'}{a_{m+1} - a_m} - 1 \tag{7}$$

are discussed. Figure 7 shows our results for Δ_m at 70 K together with those obtained for the Lennard-Jones system at 57 K (see Ref. 6). As can be seen from Fig. 7, there are not only large quantitative differences between our model and the Lennard-Jones system, but also *qualitative* differences: for $m\geq 2$ in our system the distances between the layers are *smaller*, and in the Lennard-Jones system, *larger* than in the bulk of the crystal. The correc-

tions due to the different temperatures for which the calculations have been performed would strengthen the differences between the two systems. Furthermore, the results for the lowest temperature show that the relaxation of our system is *negative* (contraction of the system) and in the case of the Lennard-Jones system it is *positive* (expansion of the system).

C. Structure and displacements parallel to the surface

In Sec. III A we studied the structure perpendicular (z direction) to the surface by means of the single-particle distribution function $g_1(z)$. The points in the x,y plane of layer m are equivalent and, therefore, the relative distances between the particles are relevant. Thus, it is instructive to study the structure parallel (x,y directions) by means of the *pair correlation function,* i.e., the probability distribution for the *distances* (with respect to the x,y coordinates) between *two* particles. Let us denote in the following the pair correlation function with $g_2(r)$, where r is the relative distance between two particles with respect to the x,y coordinates. $g_2(r)$ has been simply computed by means of the coordinates x_i,y_i of all particles which belong to layer m and is given by

$$g_2(r)=\frac{1}{2\pi r\,\Delta r}\frac{n(r,\Delta r)}{\rho}\ , \tag{8}$$

where ρ is the two-dimensional macroscopic density of layer m, and $n(r,\Delta r)$ is the density in the two-dimensional spherical shell around a particle having the radii r and $r+\Delta r$. The z coordinates of the particles are not considered in $g_2(r)$, but are in $g_1(z)$ (see Fig. 4). Results for $g_2(r)$ for various layers m are represented in Figs. 8–10. It can be seen from Figs. 8–10 that $g_2(r)$ for the innermost ($m=6$) layer agrees very well for all temperatures (7, 70, and 102 K) with that in the bulk of the crystal.

The results for $g_2(r)$ for the outermost ($m=1$) layer at $T=7$ K agrees well with those for the innermost ($m=6$) layer. Thus, at $T=7$ K there are no (or almost no) structural effects *parallel* to the surface. This is consistent with the fact that the mean-square displacements

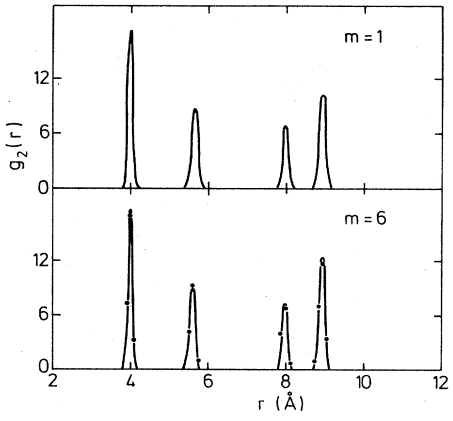

FIG. 8. Pair correlation function $g_2(r)$ parallel to the surface ($T=7$ K): ——, surface calculation; · · · ·, bulk calculation.

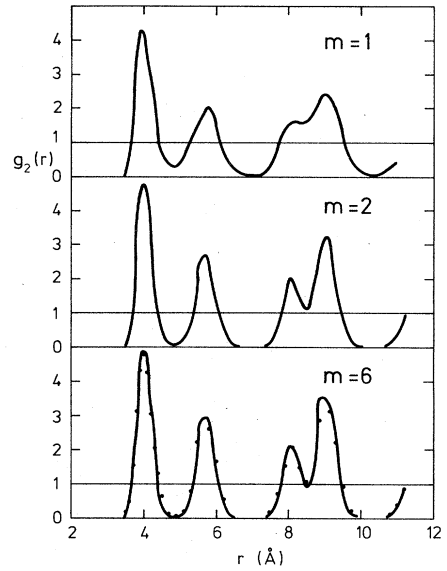

FIG. 9. Pair correlation function $g_2(r)$ parallel to the surface ($T=70$ K): ——, surface calculation; · · · ·, bulk calculation.

parallel to the surface are almost independent of m. In contrast to this behavior we found in Sec. II A that in the calculation for 7 K the single-particle distribution function $g_1(z)$ and the mean-square displacements *perpendicular* to the surface vary strongly with m (see Figs. 4 and 5).

In the calculation for $T=70$ K we observe in $g_2(r)$ relatively large effects; the peaks of $g_2(r)$ of layer $m=1$ are broadened and their heights are reduced in comparison to those of layer $m=6$ (see Fig. 9). The mean-square amplitude parallel to the surface is approximately 125% larger for layer $m=1$ than for layer $m=6$. $g_2(r)$ for layer

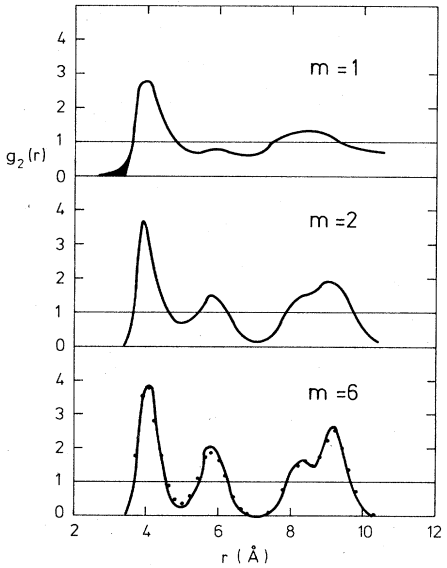

FIG. 10. Pair correlation function $g_2(r)$ parallel to the surface ($T=102$ K): ——, surface calculation; · · · ·, bulk calculation.

$m=2$ already agrees well with that of layer $m=6$ (see Fig. 9). Thus, at $T=70$ K only the structure of the outermost layer is distinctly disturbed in the x,y plane.

In the calculation for $T=102$ K (see Fig. 10) a periodic structure parallel to the surface for layer $m=1$ can hardly be recognized; in Fig. 11 three-dimensional plots for the outermost layer at 7, 70, and 102 K illustrate by comparison the degree of disorder at $T=102$ K: Although the temperature is still 14 K below the melting point, the outermost layer is extensively disordered. In particular, it can be seen from Fig. 11 that not all the particles are arranged side by side but also one upon the other, leading to the "black" area in $g_2(r)$ (see Fig. 10, $m=1$); due to the relatively small energy of the particles at $T=102$ K this "black" area in $g_2(r)$ could not be occupied in the case of a *pure* two-dimensional layer, i.e., a layer without degree of freedom perpendicular to the surface.

The mean-square displacement in the calculation for $T=102$ K shows a *singularity* parallel to the surface for $m=1$ (see Fig. 5), and this situation indicates a *diffusion process* in the x,y plane. We have determined the diffusion coefficient D for the outermost layer by means of the mean-square amplitudes $\langle r^2(t)\rangle$ parallel to the surface as a function of time. $\langle r^2(t)\rangle$ can be expressed by the VAF [defined by Eq. (3)] as follows:[20]

$$\langle r^2(t)\rangle=\frac{4k_BT}{m}\int_0^t(t-s)\psi(s)ds\ , \tag{9}$$

where m is the mass of the particles. With the asymptotic form

$$\lim_{t\to\infty}\langle r^2(t)\rangle=4Dt+\text{const}\ , \tag{10}$$

we can estimate the diffusion coefficient D from our MD data. We have calculated $\langle r^2(t)\rangle$ from the MD data by

$$\langle r^2(t)\rangle=\frac{1}{N_\tau}\frac{1}{N_l}\sum_{j=1}^{N_\tau}\sum_{i=1}^{N_l}[\mathbf{r}_i(t+\tau_j)-\mathbf{r}_i(\tau_j)]^2\ , \tag{11}$$

where N_τ is the number of time origins and N_l is the number of particles in the outermost layer. N_τ was chosen to be 200. With $N_l=50$ (see Sec. II) we obtain a statistical error of 1%. The results for $\langle r^2(t)\rangle$ are represented in Fig. 12. On the basis of Eq. (10), we have estimated D from the slope of the linear part of $\langle r^2(t)\rangle$ given in Fig. 12, and we obtained for D a value of 0.85×10^{-5} cm^2/sec, which is also a typical value for *liquids*.

Because D is so large and the structure of the layer is disordered at 102 K (see Figs. 10 and 11), we may conclude that the outermost layer shows the effect of *surface premelting* already investigated for Lennard-Jones systems.[4,21] In Ref. 21 the diffusion process has not been studied, and in Ref. 4 the long-time gradient for $\langle r^2(t)\rangle$ is immeasurably small on the MD scale and, in our opinion, one is hardly able to recognize a diffusive motion. This means that the observed premelting in our system is obviously much more pronounced than in the case of the Lennard-Jones system studied in Ref. 4. It is not straightforward to understand physically why Barker's potential shows stronger premelting phenomena than the Lennard-Jones system given in Ref. 4.

The diffusive motion parallel to the surface in the outermost layer indicates that *nonlinear* effects to $T=102$ K should be very pronounced. In fact, due to the anharmonicities parallel to the surface the spectrum of the phonon density of states $f(\omega)_{||}$ in the calculation for $T=102$ K (see Fig. 13) is shifted to lower frequencies with respect to $f(\omega)_{||}$ at 7 K. In particular, it can be seen from Fig. 13 that $f(\omega=0)_{||}$ at $T=102$ K is not zero, which is consistent with the fact that the particles perform a diffusive motion in the x,y plane. $f(\omega)_{||}$ is connected to the diffusion coefficient D by[20]

$$f(\omega=0)_{||}=\frac{2}{\pi}\frac{m}{k_BT}D\ , \tag{12}$$

and the numerical value obtained from $f(\omega=0)_{||}$ agrees well with that we have estimated from $\langle r^2(t)\rangle$. A more detailed discussion concerning surface phonons (in particular, the phonons perpendicular to the surface) is given in Ref. 22.

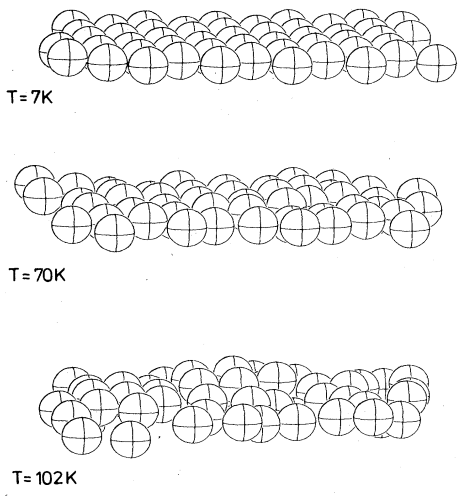

FIG. 11. Three-dimensional plots for the outermost layer at 7, 70, and 102 K.

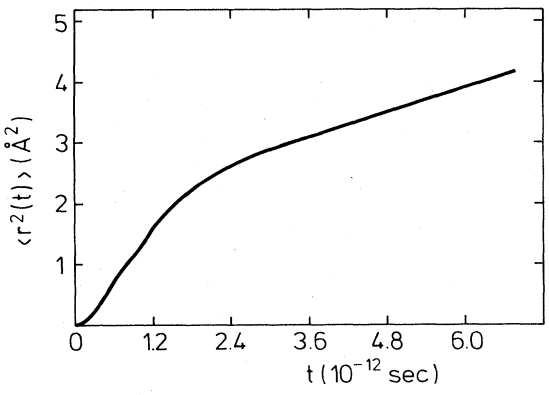

FIG. 12. Mean-square amplitudes parallel to the surface as a function of time ($T=102$ K).

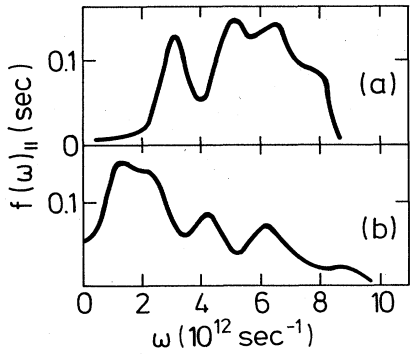

FIG. 13. Phonon density of states parallel to the surface. (a) $T=7$ K and (b) $T=102$ K.

IV. SUMMARY

In order to carry out a first-principles calculation of surface properties, it is necessary to have an accurate knowledge of the atomic interactions. All MD calculations on *noble-gas* surfaces reported in the literature have been done exclusively with Lennard-Jones potentials. In our MD calculations for krypton we have used Barker's potential. This potential should be more realistic than the Lennard-Jones potential because it undoubtedly correlates accurately a much wider range of experimental data. Although there are no *qualitative* differences between Barker's potential and the Lennard-Jones potential, we found that the differences between the two potentials not only give rise to quantitative differences in the results of surface properties, but also to *qualitative* effects.

The structure of the layers has been studied by means of the single-particle distribution function and the pair correlation function. Whereas the results for the *innermost* layer of the model agree very well with the corresponding data of the bulk, there are relatively large effects in the *outermost* layer. This is also the case for the mean-square displacements $\langle u^2 \rangle$: $\langle u^2 \rangle$ is much larger in the outermost layer than in the bulk of the crystal. For example, in the calculation for $T=7$ K the mean-square displacement perpendicular to the surface is approximately 10 times larger than in the bulk. For $T=102$ K we observe the effect of surface premelting: the outermost layer is disordered and the particles perform a diffusive motion parallel to the surface, and the diffusion coefficient D is comparable to that in liquids. The effect of premelting in our realistic system is obviously much more pronounced than in the case of Lennard-Jones systems.[4]

ACKNOWLEDGMENTS

The author would like to thank Professor F. W. de Wette and Dr. P. v. Blanckenhagen for helpful discussions.

[1]F. W. de Wette, in *Interatomic Potentials and Simulation of Lattice Defects,* edited by P. G. Gehlen, J. R. Bealer, Jr., and R. I. Jaffee (Plenum, New York, 1972), pp. 653–671.
[2]R. K. Kalia, P. Vashishta, and S. D. Mahanti, Phys. Rev. Lett. **49**, 676 (1982).
[3]F. F. Abraham, S. W. Koch, and W. E. Rudge, Phys. Rev. Lett. **49**, 1830 (1982).
[4]J. Q. Broughton and L. V. Woodcock, J. Phys. C **11**, 2743 (1978).
[5]J. A. Barker *et al.*, J. Chem. Phys. **61**, 3081 (1974).
[6]R. E. Allen, F. W. de Wette, and A. Rahman, Phys. Rev. **179**, 887 (1969).
[7]W. Schommers and P. v. Blanckenhagen, in Proceedings of the Interdisciplinary Surface Science Conference, Warwick (1983) [Vacuum **33**, 733 (1983)].
[8]A. Rahman, in *Correlation Functions and Quasi Particle Interactions in Condensed Matter,* edited by J. W. Halley (Plenum, New York, 1978), p. 417.
[9]G. L. Pollack, Rev. Mod. Phys. **36**, 74B (1964).
[10]W. Schommers, Phys. Rev. A **16**, 327 (1977).
[11]C. Hoheisel, Phys. Rev. A **23**, 1998 (1981).
[12]W. Schommers, Phys. Rev. A **22**, 2855 (1980).
[13]B. M. Axilrod and E. Teller, J. Chem. Phys. **11**, 229 (1943).
[14]*Rare Gas Solids,* edited by M. L. Klein and J. A. Venables (Academic, New York, 1977).
[15]J. Skalyo, Y. Endok, and G. Shirane, Phys. Rev. B **9**, 1797 (1974).
[16]T. H. K. Barron and M. L. Klein, Proc. Phys. Soc. London **85**, 533 (1965).
[17]A. Teitsma and P. A. Egelstaff, Phys. Rev. A **21**, 367 (1980).
[18]R. A. Aziz, Mol. Phys. **38**, 177 (1979).
[19]R. E. Allen and F. W. de Wette, Phys. Rev. **179**, 873 (1969).
[20]P. A. Egelstaff, in *An Introduction to the Liquid State* (Academic, London, 1967).
[21]R. M. J. Cotterill, Philos. Mag. **32**, 1203 (1975).
[22]W. Schommers and P. v. Blanckenhagen (unpublished).